Dalton Transactions

Exploring Opportunities for Tuning Phenyltris(pyrazol-1-yl)borate Donation by Varying the Extent of Phenyl Substituent Fluorination

Journal:	*Dalton Transactions*
Manuscript ID	DT-ART-03-2023-000735.R1
Article Type:	Paper
Date Submitted by the Author:	24-Mar-2023
Complete List of Authors:	Fischer, Paul; Macalester College, Chemistry Roe, Charley; Macalester College, Chemistry Stephenson, Jasmine; Macalester College, Chemistry Dunscomb, Rachel J; University of Minnesota, Chemistry Carthy, Camille; Lafayette College, Chemistry Nataro, Chip; Lafayette College, Chemistry Young, Jr., Victor; University of Minnesota, Chemistry

SCHOLARONE™
Manuscripts

Exploring Opportunities for Tuning Phenyltris(pyrazol-1-yl)borate Donation by Varying the Extent of Phenyl Substituent Fluorination

Paul J. Fischer,[*,a] Charley B. Roe,[a] Jasmine N. Stephenson,[a] Rachel J. Dunscomb,[b] Camille L. Carthy,[c] Chip Nataro[c] and Victor G. Young, Jr.[b]

[a]Department of Chemistry, Macalester College, 1600 Grand Avenue, Saint Paul, MN 55105, USA

[b]Department of Chemistry, University of Minnesota, 207 Pleasant Street SE, Minneapolis, MN 55455, USA

[c]Department of Chemistry, Lafayette College, 730 High Street, Easton, PA 18042, USA

[*]Email: fischer@macalester.edu; Tel: +1-651-696-6585

Abstract

The importance of electron deficient Tp ligands motivates the introduction of electron-withdrawing substituents into the scorpionate framework. Since perfluorophenyltris(pyrazol-1-yl)borate affects significant anodic shifts in half-cell potentials in their metal complexes relative those of phenyltris(pyrazol-1-yl)borate analogues, the tuning opportunities achieved using 3,4,5-trifluorophenyl- and 3,5-bis(trifluoromethyl)phenyl(pyrazol-1-yl)borates were explored. Bis(amino)boranes $((3,4,5\text{-F})C_6H_2)B(NMe_2)_2$ and $((3,5\text{-}CF_3)C_6H_3)B(NMe_2)_2$ are precursors to fluorinated tris(pyrazol-1-yl)phenylborates. Thallium salts of these scorpionates exhibit bridging asymmetric κ^3-*N*,*N*,*N* coordination modes consistent with the reduced π-basicity of the fluorinated phenyl substituents relative those of other structurally characterized tris(pyrazol-1-yl)phenylborates. While a comparative analysis of the spectral and X-ray crystallographic data

for classical Mo(0), Mo(II), Mn(I), Fe(II) and Cu(II) complexes of $[((3,4,5\text{-F})C_6H_2)Bpz_3]^-$ and $[((3,5\text{-}CF_3)C_6H_3)Bpz_3]^-$ could not differentiate these ligands with respect to their metal-based electronic impacts, cyclic voltammetry suggests that 3,4,5-trifluorophenyl- and 3,5-bis(trifluoromethyl)phenyl(pyrazol-1-yl)borates affect similar anodic shifts within their metal complexes, with coordination of $[((3,5\text{-}CF_3)C_6H_3)Bpz_3]^-$ rendering metal centers more difficult to oxidize, and sometimes even more difficult to oxidize than their $[C_6F_5Bpz_3]^-$ analogues. These data suggest that the extent of phenyl substituent fluorination necessary to minimize metal center electron-richness in phenyltris(pyrazol-1-yl)borate complexes cannot be confidently predicted.

Introduction

Vigorous employment of tris(pyrazol-1-yl)borates continues within essentially every inorganic chemistry subfield, including coordination chemistry of transition metals and main group elements, materials chemistry, organometallic chemistry, ligand design and catalysis.[1] Fluorinated tris(pyrazol-1-yl)borates represent a Tp ligand class that has gained prominence, particularly with Group XI metals, in stabilizing rare species such as π-acetylene complexes ($[HB(3,5\text{-}(CF_3)_2Pz)_3]M(C_2H_2)$, $[HB(3\text{-}(CF_3)\text{-}5\text{-}(Ph)Pz)_3]M(C_2H_2)$ (M = Cu, Ag)),[2] heterobimetallics with iron pentacarbonyl ligands (*e.g.*, $[HB(3,5\text{-}(CF_3)_2Pz)_3]Ag\text{-}Fe(CO)_5$[(3)]), π-ethylene complexes ($[HB(3\text{-}(CF_3)\text{-}5\text{-}(CH_3)Pz)_3]M'(C_2H_4)$ (M' = Cu, Ag, Au),[4] $[HB(3,4,5\text{-}(CF_3)_3Pz)_3]M(C_2H_4)$[5]), complexes of 1-azidoadamantane ($[HB(3,5\text{-}(CF_3)_2Pz)_3]CuNNN(1\text{-}Ad)$, $[HB(3,5\text{-}(CF_3)_2Pz)_3]AgN(1\text{-}Ad)NN$[6]) and a silver(I) complex of dimethyl diazomalonate ($[HB(3,5\text{-}CF_3)_2Pz)_3]Ag[OC(OCH_3)]_2CN_2$[(7)]). Fluorinated tris(pyrazol-1-yl)borates also support catalytically active complexes including $[HB(3,5\text{-}(CF_3)\text{-}4\text{-}(Br)Pz)_3]Cu(NCCH_3)$, that catalyzes $:CHCO_2Et$ insertion into methane C–H bonds,[8] and $\{[HB(3,5\text{-}(CF_3)_2Pz)_3]Zn(NCCH_3)_2\}ClO_4$ that similarly catalyzes alkane C–H functionalization.[9] The weakly donating nature of these ligands

engenders these metal-based chemical properties, and exploration of borates with alternate fluorination profiles impacting the five-membered C_3N_2 rings (*e.g.*, $[HB(3\text{-}(C_2F_5)\text{-}5\text{-}(CH_3)Pz)_3]^-$ [(10)], perfluorinated hydrotris(indazol-1-yl)borates[11]) is ongoing.

Tris(pyrazol-1-yl)borate donation can also be modulated by changing the nondonor boron substituent, which is hydrogen (*i.e.*, $[HBpz_3]^-$) in the vast majority of complexes. While pyrazol-1-yl ring fluorination will affect a greater electronic impact at coordinated metals relative to that leveraged by nondonor boron substituent fluorination (due to the electronic insulation from the pyrazolyl groups because of the sp^3 boron atom hybridization), the heightened interest in weakly donating tris(pyrazol-1-yl)borates motivates studies to ascertain further ligand tuning opportunities. A foundational inaugural entry was Wagner's investigation of tris(pyrazol-1-yl)perfluorophenylborate.[12] Five pairs of perfluorophenyl- and phenyl-substituted tris(pyrazol-1-yl)borate complexes ($(C_6R'_5BPz_3)_2Fe$, $(C_6R'_5Bpz_3)_2Cu$, $(C_6R'_5Bpz_3)Mn(CO)_3$, $K[(C_6R'_5Bpz_3)Mo(CO)_3]$, $(C_6R'_5Bpz_3)Mo(CO)_2$(2-methallyl) (R' = F, H)) were comparatively examined. While the fluorination impact could not be distinguished at these metals via analyses of X-ray crystallographic and IR spectroscopic data, significant differences between the half-cell potentials of the fluorinated and non-fluorinated species were assessed. Switching from a C_6H_5 to a C_6F_5 substituent renders the respective metal center of its $C_6R'_5Bpz_3$ complex more difficult to oxidize, forecasting practical utility leveraged by this Tp design strategy.

A query associated with this tris(pyrazol-1-yl)phenylborate design approach is whether donation can be rationally tuned by varying the extent of phenyl substituent fluorination. To this end complexes containing 3,4,5-trifluorophenyl- and 3,5-bis(trifluoromethyl)phenyltris(pyrazol-1-yl)borates have been prepared. While 3,4,5-trifluorophenyltris(pyrazol-1-yl)borate would be expected to render κ^3-*N*,*N*,*N* bound metals more electron-rich than Wagner's perfluorophenyltris(pyrazol-1-yl)borate, the impact of 3,5-bis(trifluoromethyl)phenyltris(pyrazol-

1-yl)borate is not straightforward to predict. The relative Lewis acidity of $B(C_6F_5)_3$ and $B(3,5\text{-}(CF_3)C_6H_3)_3$ has been disputed, with the ranking dependent on the assessment methodology.[13,14] While the relative group electronegativity of the C_6F_5 and $3,5\text{-}(CF_3)C_6H_3$ substituents is just one factor in determining the Lewis acidities of these neutral boranes, an assessment of 3,5-bis(trifluoromethyl)phenyltris(pyrazol-1-yl)borate is meritorious independently to inform the important development of new fluorinated tris(pyrazol-1-yl)borates.

Results and Discussion

Ligand Syntheses and Characterization. The bis(amino)boranes $((3,4,5\text{-}F)C_6H_2)B(NMe_2)_2$ (**1**) and $((3,5\text{-}CF_3)C_6H_3)B(NMe_2)_2$ (**2**) are convenient precursors for the targeted fluorinated tris(pyrazol-1-yl)phenylborates (Scheme 1). Reactions of $BrB(NMe_2)_2$ and $((3,4,5\text{-}F)C_6H_2)MgBr$ and $((3,5\text{-}CF_3)C_6H_3)MgBr$ result in solutions from which colorless liquids **1** and **2** can be obtained in good yields (**1**: 73%; **2**: 83%) by vacuum distillation (**1**: 82-84 °C, 3 torr; **2**: 75-77 °C, 3 torr). While elevated temperatures are employed to purify these boranes, **2** suffers thermal instability upon ambient temperature storage, but can be confidently stored at least one week at -40 °C as a solid. The ^{11}B NMR chemical shifts of **1** and **2** in C_6D_6 are identical (δ 31.3 (s)), ~3 ppm downfield that of $(C_6F_5)B(NMe_2)_2$ (δ (C_6D_6) 28.4 (s)) but upfield that of $PhB(NMe_2)_2$ (δ (C_6D_6) 32.4 (s)).[12] The ^1H NMR methyl resonances of these fluorinated phenyl boranes in C_6D_6 vary by <0.1 ppm (δ: **1**: 2.37 (s), **2**: 2.31 (s), $C_6F_5B(NMe_2)_2$: 2.39 (s)). These single methyl resonances of **1**, **2** and

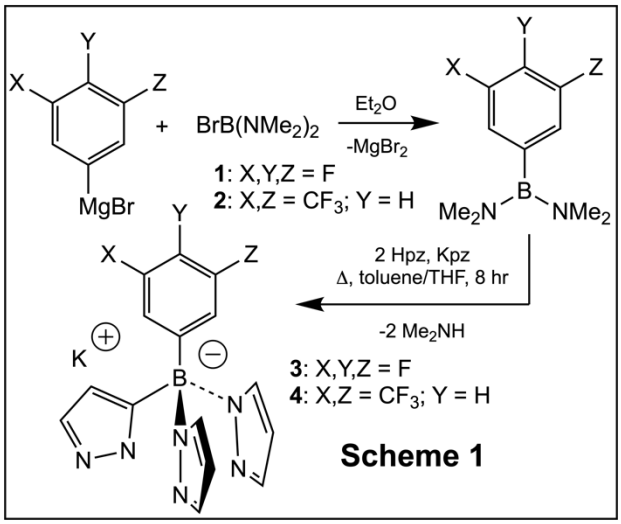

Scheme 1

$C_6F_5B(NMe_2)_2$ suggest rapid rotation of the NMe_2 substituents about the B–N bonds relative the NMR timescale, consistent with insignificant N–B π bonding. This bonding assessment is further supported by the single $^{13}C\{^1H\}$ NMR methyl resonances of **1** (δ 50.0 (s)), **2** (δ 40.9 (s)) and $C_6F_5B(NMe_2)_2$ (δ 40.1 (s)).

Reactions of bis(amino)boranes **1** and **2** with pyrazole and potassium pyrazolate in toluene:THF affect dimethylamine elimination and high yield formation of K[((3,4,5-F)C_6H_2)Bpz_3] (**3**, 91%) and K[((3,5-CF_3)C_6H_3)BPz_3] (**4**, 93%). Direct extension of the Wagner K[$C_6F_5BPz_3$] synthetic protocol,[12] in which neat pyrazole and potassium pyrazolate are added simultaneously to a toluene solution of $(C_6F_5)B(NMe_2)_2$, afforded multiple boron-containing products when employed analogously with **1** and **2**. The optimum **3**/**4** procedure required stirring **1** and **2** with pyrazole for ~2 hours prior to potassium pyrazolate introduction. Crude samples of **3** and **4** contain toluene; extended heating under vacuum is required to obtain solvent-free solids with formulations supported by combustion analyses. The ^{11}B NMR chemical shifts of **3** (δ 0.71 (s)) and **4** (δ 0.95 (s)) in DMSO-d^6 are slightly downfield that of K[$C_6F_5Bpz_3$] (δ -1.8 (s)) in C_4D_8O.[12] The three unique pyrazolyl hydrogen environments of **3** and **4** are well-resolved via separate resonances that integrate to 3H each in DMSO-d^6 solution (^1H NMR **3**: δ 7.49 (H3/5), 6.75 (H3/5), 6.07 (H4); **4**: δ 7.52 (H3/5), 6.73 (H3/5), 6.10 (H4)) in contrast to that measured for K[$C_6F_5Bpz_3$] in C_4D_8O solution (^1H NMR δ 7.43 (6H, H3/5), 6.05 (3H, H4).[12]

While **3** and **4** are heretofore excellent sources of these anions for installation at transition metals, difficulty in obtaining single crystals of these potassium salts motivated metathesis attempts. Thallium acetate was a convenient reagent for potassium/thallium exchange for formation of Tl[((3,4,5-F)C_6H_2)Bpz_3] (**5**) and Tl[((3,5-CF_3)C_6H_3)Bpz_3] (**6**). The ^{11}B NMR

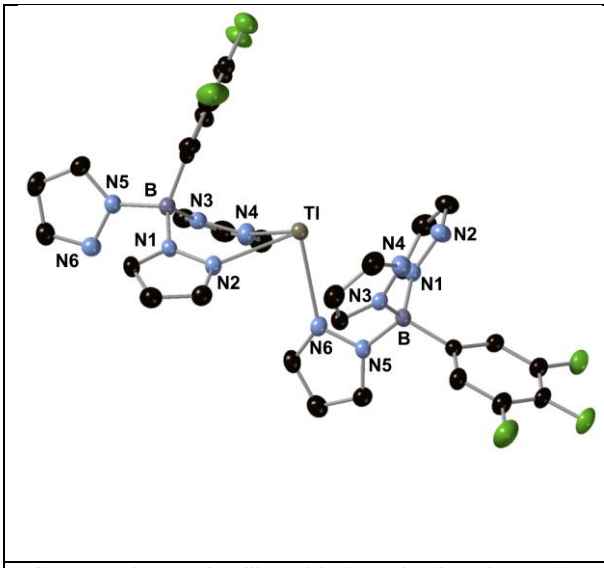

Fig. 1 Thermal ellipsoid (50%) drawing of **5**. Selected bond lengths (Å) and angles (°) Tl–N(2) = 2.574(3), Tl–N(4) = 2.595(3), Tl–N(6) = 2.741(3), N(1)–B–N(3) = 111.5(2), N(5)–B–N(3) = 105.5(3), N(5)–B–N(1) = 105.8(3), N(2)–Tl–N(4) = 71.33(9), N(2)–Tl–N(6) = 84.67(8), N(4)–Tl–N(6) = 79.76(9)

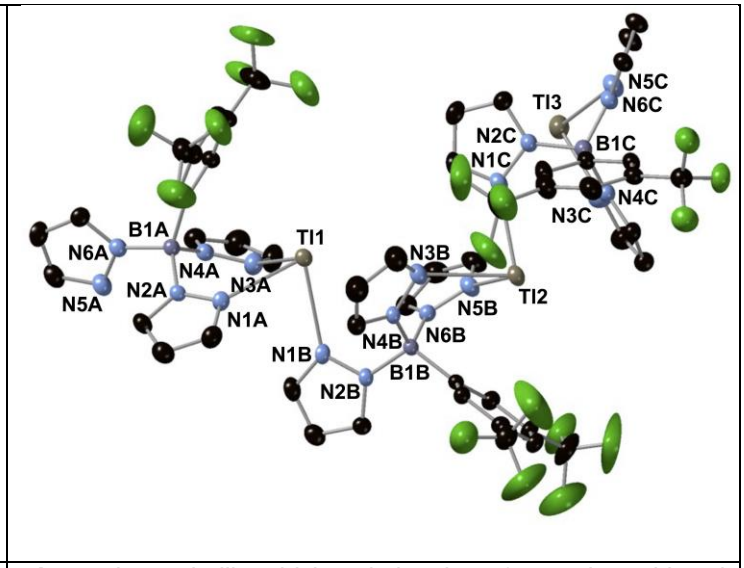

Fig. 2 Thermal ellipsoid (50%) drawing of **6**. Selected bond lengths (Å) and angles (°) Tl(1)–N(1A) = 2.583(2), Tl(1)–N(3A) = 2.605(3), Tl(1)–N(1B) = 2.712(3), Tl(2)–N(5B) = 2.550(2), Tl(2)–N(3B) = 2.689(2), Tl(2)–N(1C) = 2.631(3), Tl(3)–N(3C) = 2.608(3), Tl(3)–N(5C) = 2.623(2), Tl(3)–N(5A) = 2.756(3). Ave N–Tl–N (same anion) = 71.5(8), Ave N–Tl–N (different anions) = 82(4). Ave N–B–N (involving rings with shorter Tl–N bonds) = 107(1), Ave N–B–N (involving bridging rings with longer Tl–N bonds) = 110.8(8)

chemical shifts of **5** (δ 0.94 (s)) and **6** (δ 1.17 (s)) in C_4D_8O and separate pyrazolyl hydrogen environments (^{1}H NMR **5**: δ 7.59 (H3/5), 7.32 (H3/5), 6.20 (H4); **6**: δ 7.61 (H3/5), 7.32 (H3/5), 6.22 (H4)) are slightly downfield those **3** and **4**. Thermal ellipsoid drawings of **5** (Fig. 1) and **6** (Fig. 2) exhibit polymeric connectivity in the solid-state. Two pyrazolyl rings of one anion and one of another establish a bridging asymmetric κ^3-*N,N,N* coordination mode in **5** (Tl–N(2) = 2.574(3) Å, Tl–N(4) = 2.595(3) Å, Tl–N(6) = 2.741(3) Å), that possesses one unique thallium center. The N–B–N angle associated with the chelating pyrazolyl rings is larger (N(1)–B–N(3) = 111.5(2)°) than those angles associated with the ring participating in the bridging interaction

(N(5)–B–N(3) = 105.5(3)°, N(5)–B–N(1) = 105.8(3)°). The molecular structure of **6** is similar but with three unique thallium centers. The average bridging Tl–N separation (2.70(6) Å) and shorter chelating Tl–N distance (2.61(5) Å) are statistically indistinguishable.

The bridging thallium binding mode of **5** and **6** is different from that in the two other crystallographically characterized thallium tris(pyrazol-1-yl)phenylborates, Parkin's Tl[PhB(3-(^{t}Bu)pz)$_3$][15] and Theopold's Tl[PhB(3-(Fc)pz)$_3$] (Fc = ferrocenyl).[16] Phenyl substituent steric bulk is hypothesized to destabilize symmetric κ^3-*N,N,N* coordination in Tl[PhB(3-(^{t}Bu)pz)$_3$], resulting in thallium being principally coordinated to two pyrazolyl groups, with Tl–N distances (2.528(3) Å, 2.585(3) Å) very similar to those chelating distances in **5** and **6**, but with tridentate coordination achieved via a π-interaction with the nitrogen bound the third pyrazolyl ring (Tl–N = 2.833(2) Å) that is rotated ~90° about the B–N bond. The thallium of Tl[PhB(3-(Fc)pz)$_3$] is similarly bound to two pyrazolyl rings (Tl–N: 2.570(4) Å, 2.592(9) Å) and engages an interaction with the phenyl substituent π-system with a shortest Tl–C distance of 2.980(1) Å to the *ipso* carbon. The additional interactions that render these tris(pyrazol-1-yl)phenylborates as putative tridentate ligands are absent in **5** and **6**, where the shortest Tl–(*ipso*-C) separations are 3.692(9) Å (**5**, Tl–C(10)) and 3.375(7) Å (**6**, Tl2–C(10B)). The lack of bulky pyrazolyl 3-substituents, coupled with the reduced π-basicity of fluorinated phenyl substituents, results in these polymeric solid-state structures of **5** and **6** that nevertheless avoid symmetric κ^3-*N,N,N* binding.

Metal Complex Synthesis and Structural Characterization. A thorough examination of 3,4,5-trifluorophenyltris(pyrazol-1-yl)borate and 3,5-bis(trifluoromethyl)phenyltris(pyrazol-1-yl)borate donation requires comparison with Wagner's analogous perfluorophenyltris(pyrazol-1-yl)borate and phenyltris(pyrazol-1-yl)borate complexes.[12] To this end, we prepared [Et$_4$N][Mo(CO)$_3$(((3,4,5-F)C$_6$H$_2$)Bpz$_3$)] (**7**), [Et$_4$N][Mo(CO)$_3$(((3,5-CF$_3$)C$_6$H$_3$)Bpz$_3$)] (**8**), (((3,4,5-

F)C_6H_2)Bpz_3)$Mo(CO)_2$(2-methallyl) (**9**), (((3,5-CF_3)C_6H_3)Bpz_3)$Mo(CO)_2$(2-methallyl) (**10**), (((3,4,5-F)C_6H_2)Bpz_3)$Mn(CO)_3$ (**11**), (((3,5-CF_3)C_6H_3)Bpz_3)$Mn(CO)_3$ (**12**), Fe(((3,4,5-F)C_6H_2)Bpz_3)$_2$ (**13**), Fe(((3,5-CF_3)C_6H_3)Bpz_3)$_2$ (**14**), Cu(((3,4,5-F)C_6H_2)Bpz_3)$_2$ (**15**) and Cu(((3,5-CF_3)C_6H_3)Bpz_3)$_2$ (**16**). These classical analogues were straightforward to synthesize with **3** as **4** as ligand sources (Scheme 2). $Mo(CO)_3(CH_3CH_2CN)_3$ was used as the precursor for **7** and **8**; isolation of tetraethylammonium salts allows $Mo(CO)_3$ unit examination without the ion-pairing present in K[$Mo(CO)_3(C_6F_5Bpz_3)$].[12] Oxidative addition of $Mo(CO)_3(C_6H_5N)_3$ with 3-bromo-2-methyl-1-propene followed by salt elimination[17] provided **9** and **10**. The manganese(I) complexes **11** and **12** were prepared via naphthalene displacement from [$Mn(C_{10}H_8)(CO)_3$][BF_4]. Treatment of **3** and **4** with $FeCl_2$ in THF provided **13** and **14**, while **15** and **16** were prepared similarly via **3**, **4** and $CuBr_2$. The formulations of **7**-**16** were verified by combustion analyses, and each was characterized by X-ray crystallography.

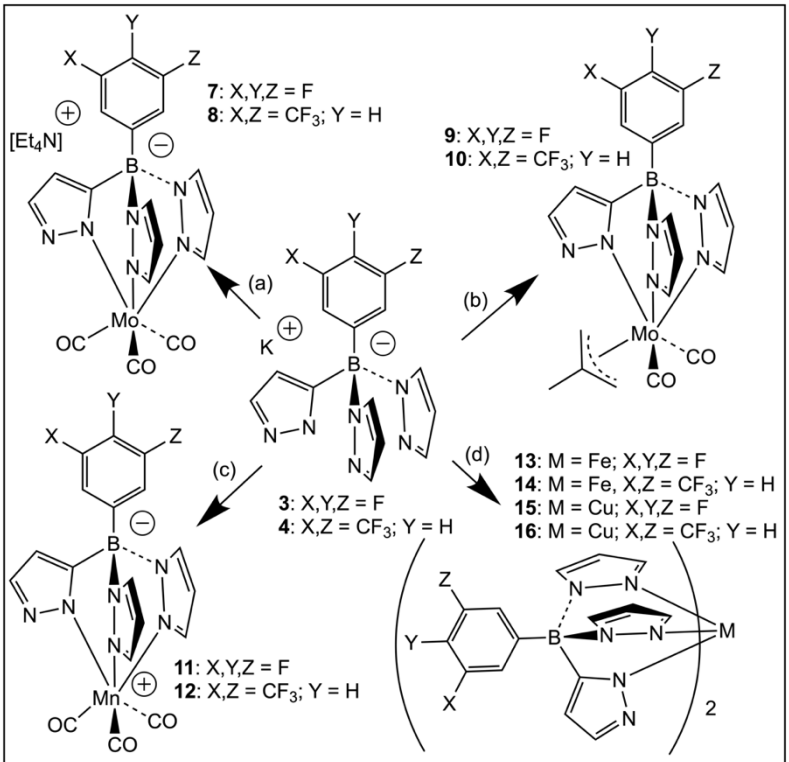

Scheme 2

Wagner found no significant differences in the structural parameters defining the metal coordination geometries between the [$PhBpz_3$]$^-$ and [$C_6F_5Bpz_3$]$^-$ analogues of **7**-**16** hence no such differences were anticipated upon analyses of the [((3,4,5-F)C_6H_2)Bpz_3]$^-$ analogues (**7**, **9**, **11**, **13**, **15**). Of more interest was whether these parameters of the [((3,5-CF_3)C_6H_3)Bpz_3]$^-$ analogues (**8**, **10**, **12**, **14**, **16**) might be

differentiated, but such tuning could not be detected with the exception of some copper coordination environment anomalies in **15** and **16**. Figures S1-S6 provide the structures of monoscorpionate complexes **7**-**12**.

The molybdenum-centered geometries of **7** and **8** are statistically identical on the basis of the average Mo–N (**7**/**8**, 2.26(3) Å), Mo–C (**7**, 1.936(3) Å; **8**, 1.933(5) Å) and C–O (**7**, 1.177(2) Å; **8**, 1.176(8) Å) distances; these parameters are indistinguishable those of [K(THF)][(PhBpz$_3$)Mo(CO)$_3$] (Mo–N: 2.26(2) Å, Mo–C: 1.94(1) Å, C–O: 1.19(1) Å).[12] A salt of [(C$_6$F$_5$Bpz$_3$)Mo(CO)$_3$]$^-$ has not been crystallographically characterized. The fluorinated phenyl substituents of **7** and **8** adopt positions nearly orthogonal one of the three pyrazolyl rings (dihedral angle C(15)–C(10)–B–N(2): **7**, 89.0(2)°; **8**, 84.3(3)°). The reduced effective steric bulk of this fluorinated substituent on the N(2) pyrazolyl ring results in smaller C(10)–B–N(2) angles (**7**, 106.92(15)°; **8**, 106.93(18)°) relative the other *ipso*-C–B–N angles (ave(**7**/**8**) = 114(1)°).

There are two complexes in the asymmetric unit of **9**, and just one in that of **10**. The η^3-2-methylallyl ligand methyl substituents are oriented into voids between pyrazolyl groups. As with the molybdenum(0) complexes **7**, **8** and [K(THF)][(PhBpz$_3$)Mo(CO)$_3$], the molybdenum(II) coordination geometries of **9**, **10**, (C$_6$F$_5$Bpz$_3$)Mo(CO)$_2$(2-methallyl) and (PhBpz$_3$)Mo(CO)$_2$(2-methallyl) are impervious to the extent of fluorination (*e.g.*, average Mo–N: **9**, 2.27(5) Å; **10**, 2.25(4) Å; (C$_6$F$_5$Bpz$_3$)Mo(CO)$_2$(2-methallyl), 2.25(2) Å; (PhBpz$_3$)Mo(CO)$_2$(2-methallyl), 2.25(4) Å).[12] While the orientation of the fluorinated phenyl substituents relative the pyrazolyl rings of **9** resemble those of **7** and **8**, the bis(3,5-trifluoromethyl)phenyl substituent of **10** exhibits a less orthogonal relationship to the N(2) pyrazolyl ring (N(2)–B–C(10)–C(15) = 76.36(17)°) resulting in relatively acute dihedral angle involving the N(6) pyrazolyl ring (N(6)–B–C(10)–C(11) = 25.9(2)°). The phenyl substituent disposition in **10** is likely governed in part by intermolecular interactions in the crystalline lattice.

Both **11** and **12** exhibit C_s symmetry. The manganese(I) coordination geometries of zwitterions **11**, **12**, $(C_6F_5Bpz_3)Mn(CO)_3$, and $(PhBpz_3)Mn(CO)_3$ again exhibit no differences (*e.g.*, average Mn–N: **11**, 2.04(2) Å; **12**, 2.04(2) Å; $(C_6F_5Bpz_3)Mn(CO)_3$, 2.06(2) Å; $(PhBpz_3)Mn(CO)_3$, 2.05(1) Å).[12] All of these lengths are shorter than the average Mn–N distances in $(HB\{3\text{-}(CF_3)pz\}_3)Mn(CO)_3$ (2.125(3) Å) and $(HB\{3,5\text{-}(CF_3)_2pz\}_3)Mn(CO)_3$ (2.122(3) Å); elongation of these distances has been attributed to weaker Tp donation on the basis of fluorination.[18] Acute N(2)–B–C(10) angles (**11**, 107.73(11)°; **12**, 106.14(17)°) are similarly present on the basis of nearly orthogonal dispositions of the fluorinated phenyl substituents relative the N(2) pyrazolyl ring with the other N–B–*ipso*-C angles being larger (Ave(**11**/**12**) = 115.0(9)°).

The iron(II) discorpionate complexes **13** and **14** are analogues of $(C_6F_5BPz_3)_2Fe$ which exhibits novel spin-crossover behavior.[19] Both **13** and **14** adopt different structures in the solid-state. In **13**, two C_i structures are present in an approximate 4:1 ratio; the major structure is displayed in Figure 3. While the iron coordination geometries of these structures (that employ equivalent iron centers) are statistically identical, with average Fe–N distances (major = 1.959(2) Å, minor = 1.98(3) Å) typical of low-spin iron(II) complexes, the primary difference is a disordered phenyl substituent orientation. While this group is approximately orthogonal the pyrazolyl group defined by N(4) in the major structure, this group is rotated in the minor structure (Fig. S7) and nearly orthogonal the pyrazolyl group defined by N(6') (analogous dihedral = 84(3)°). Four $Fe(((3,5\text{-}CF_3)C_6H_3)Bpz_3)_2$ complexes, each with C_i symmetry, are in the asymmetric unit of single crystals of **14** (Fig. S8-S11). The

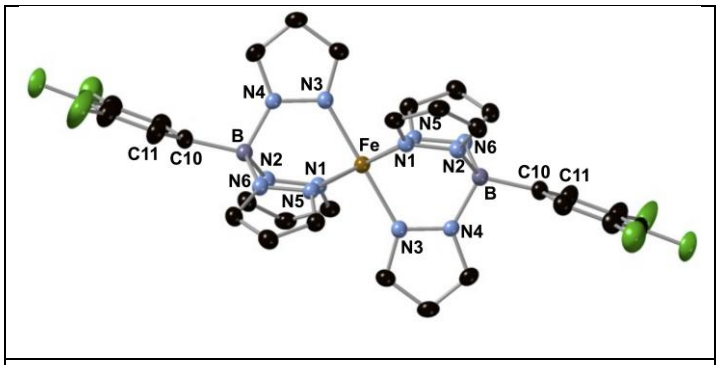

Fig. 3 Thermal ellipsoid (50%) drawing of **13** (major form). Selected bond lengths (Å) and angles (°) Fe–N(1) = 1.958(4), Fe–N(3) = 1.958(3), Fe–N(5) = 1.961(3), Ave N–Fe–N = 90(2), N(4)-B-C(10)-C(11) (Dihedral) = 84.2(4), C(10)-B-N(4) = 106.68(19), C(10)-B-N(6) = 114.9(2), C(10)-B-N(2) = 115.8(2).

iron coordination geometries of these four structures (*e.g.*, Ave Fe–N range: 1.958(9) to 1.97(1) Å; Ave N–Fe–N = 90(2)° for each) are statistically identical to those in single crystals of **13**, ($(C_6F_5BPz_3)_2Fe$ (Ave Fe–N = 1.98(2) Å) and $(PhBPz_3)_2Fe$ (Ave Fe–N = 1.97(1) Å).[12] Bis coordination of phenyltris(pyrazol-1-yl)borates with different extents of phenyl substituent fluorination has no detectable structural impact at iron(II) centers.

Wagner's $(C_6F_5Bpz_3)_2Cu$ and $(PhBpz_3)_2Cu$ exhibit different coordination geometries, with $(C_6F_5Bpz_3)_2Cu$ displaying Jahn-Teller-distorted square pyramidal copper(II), while $(PhBpz_3)_2Cu$ exhibits square planar copper(II). Two nearly identical bis(3,4,5-trifluorophenyltris(pyrazol-1-yl)borate complexes **15** are present in the asymmetric unit so just one structure (Fig. 4) will be discussed. The modestly distorted square pyramidal copper(II) in **15** features four relatively short Cu–N bonds (Ave = 1.99(1) Å) and a fifth axial nitrogen that is further away (Cu(1A)–N(3A) = 2.2679(14) Å). The plane of the sixth pyrazolyl group faces Cu(1A) but the shorter Cu(II)–N separation involving this ring (to N(11A)) is >3.1 Å. This feature of **15** is interesting when compared to that of $(C_6F_5Bpz_3)_2Cu$ where the sixth pyrazolyl substituent points away from the metal center allowing one C_6F_5 substituent to instead stay in close proximity, but with a rather long Cu(II)–(*ispo*-C) separation of 3.093(2) Å.[12] The asymmetric unit within single crystals of **16** feature two very similar complexes; one of these is in Figure 5. The six-coordinate tetragonally distorted copper(II) coordination geometry of **16** is unique from that of **15**, $(C_6F_5Bpz_3)_2Cu$ and $(PhBpz_3)_2Cu$. The average Cu(II)–N distance that defines the equatorial plane (1.998(9) Å) is significantly shorter than the symmetry equivalent

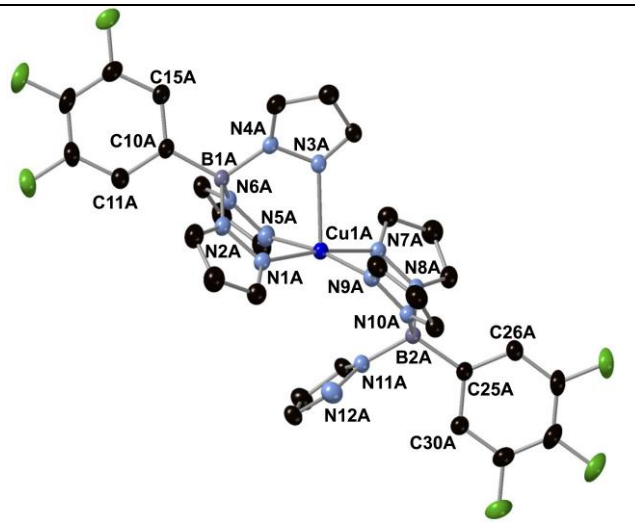

Fig. 4 Thermal ellipsoid (50%) drawing of **15**. Selected bond lengths (Å) and angles (°) Cu(1A)–N(1A) = 2.0034(14), Cu(1A)–N(5A) = 1.9865(15), Cu(1A)–N(7A) = 1.9891(14), Cu(1A)–N(9A) = 1.9884(15), Cu(1A)–N(3A) = 2.2679(14), N(5A)–Cu(1A)–N(7A) = 93.00(6), N(9A)–Cu(1A)–N(1A) = 90.15(6), N(9A)–Cu(1A)–N(7A) = 88.49(6), N(5A)–Cu(1A)–N(1A) = 87.15(6), N(5A)–Cu(1A)–N(3A) = 85.52(6), N(1A)–Cu(1A)–N(3A) = 90.05(6), N(7A)–Cu(1A)–N(3A) = 97.91(5), N(9A)–Cu(1A)–N(3A) = 103.01(6).

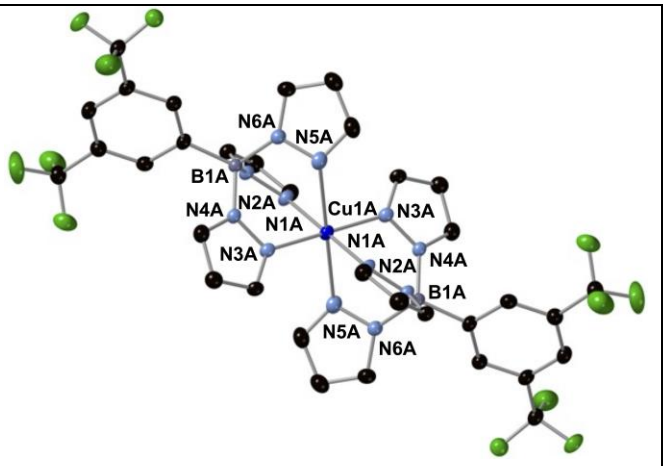

Fig. 5 Thermal ellipsoid (50%) drawing of **16**. Selected bond lengths (Å) and angles (°) Cu(1A)–N(3A) = 1.990(2), Cu(1A)–N(1A) = 2.006(2), Cu(1A)–N(5A) = 2.485(3), Ave equatorial N–Cu(1A)–N = 90(2), Ave (axial) N–Cu(1A)–N = 90(7).

axial Cu(1A)–N(5) separations (2.485(3) Å). It is highly unlikely that the distinctly different copper(II) coordination environments in **15**, **16**, $(C_6F_5Bpz_3)_2Cu$ and $(PhBpz_3)_2Cu$ in the solid-state are governed by differences in the donor capabilities of 3,4,5-trifluorophenyl-, 3,5-bis(trifluoromethyl)phenyl-, pentafluorophenyl and phenyltris(pyrazol-1-yl)borates. These structural differences more likely reflect varying impacts of these phenyl substituents during crystal packing coupled with the flexibility of copper(II) to adopt alternate coordination geometries.

Comparison of the Donor Strengths. Wagner employed infrared ν(CO) spectroscopy and cyclic voltammetry to assess the electronic impact of metals bound to $[C_6F_5Bpz_3]^-$ and $[PhBpz_3]^-$. The corresponding IR data and ^{13}CO NMR chemical shifts for **7**-**12** and Wagner's

analogues[12] are in Table 1. While the ^{13}CO NMR chemical shifts for each analogous set are essentially identical, the difference in matrix for the solid-state infrared spectroscopic measurements complicates direct comparison of the carbonyl stretching frequencies. That

Table 1: Carbonyl Spectroscopic Data

	IR ν_{max}(CO)/cm^{-1}	IR ν_{max}(CO) Ave/cm^{-1}	^{13}C NMR δ(CO)/ppm	
7	1892, 1760, 1743[a]	1798	231.8[c]	this work
8	1894, 1769, 1749, 1745[a]	1789	231.8[c]	this work
K[Mo(CO)$_3$(PhBpz$_3$)]	1885, 1765, 1742[b]	1797	232.0[d]	ref. 12
K[Mo(CO)$_3$(C$_6$F$_5$Bpz$_3$)]	1889, 1761, 1747[b]	1799	232.0[d]	ref. 12
9	1940, 1851[a]	1896	228.2[d]	this work
10	1935, 1842[a]	1889	228.2[d]	this work
(PhBpz$_3$)Mo(CO)$_2$(2-methallyl)	1935, 1836[b]	1886	228.5[d]	ref. 12
(C$_6$F$_5$Bpz$_3$)Mo(CO)$_2$(2-methallyl)	1939, 1851[b]	1895	228.4[d]	ref. 12
11	2032, 1936, 1923[a]	1964	222.3[d]	this work
12	2032, 1934, 1917[a]	1961	222.3[d]	this work
(PhBpz$_3$)Mn(CO)$_3$	2033, 1944, 1906[b]	1961	not obs.	ref. 12
(C$_6$F$_5$Bpz$_3$)Mn(CO)$_3$	2034, 1950, 1912[b]	1965	not obs.	ref. 12

[a]Nujol mull, [b]KBr pellet, [c]CD$_3$CN, [d]C$_4$D$_8$O

said, the IR spectra suggests modestly increased donation from phenyltris(pyrazol-1-yl)borate and slightly less π-backbonding into the carbonyl ligands from the fluorinated-phenyl Tp ligands. The similarity of the ν(CO) infrared spectra (and similar average CO stretching frequencies for each complex) render 3,4,5-trifluorophenyltris(pyrazol-1-yl)borate, perfluorophenyltris(pyrazol-1-yl)borate and 3,5-bis(trifluoromethyl)phenyltris(pyrazol-1-yl)borate impossible to differentiate, and rational tuning impossible to discern.

Electrochemical data for **9**-**14** and their phenyltris(pyrazol-1-yl)borate and perfluorophenyltris(pyrazol-1-yl)borate analogues[12] are in Table 2. Half-cell potentials of **9** (Fig. S12) and **10** (Fig. S13) were obtained in contrast with the irreversible oxidation of (C$_6$F$_5$Bpz$_3$)Mo(CO)$_2$(2-methallyl) and the quasireversible oxidation of (PhBpz$_3$)Mo(CO)$_2$(2-methallyl) measured by Wagner.[12] The manganese(I) complexes **11** (Fig. S14) and **12** (Fig. S15) exhibited chemically reversible oxidations, with complete chemical and electrochemical reversibility observed at scan rates greater than 0.6 V s^{-1}. Wagner reported irreversible redox

(and peak anodic potentials) for $(PhBpz_3)Mn(CO)_3$ and $(C_6F_5Bpz_3)Mn(CO)_3$ at 0.1 V s^{-1}.[12] At the same scan rate, analogues **11** (Fig. S16) and **12** (Fig. S17) displayed return reduction waves, with i_r/i_f values of 0.45 and 0.33 respectively. Chemically reversible oxidations are observed for **13** (Fig. S18), **14** (Fig. S19), $(PhBpz_3)_2Fe$ and $(C_6F_5Bpz_3)_2Fe$. These iron(II) complex data are the most reliable for comparing the electronic impact of these four ligands since all exhibit half-cell potentials; comparison of half-cell and peak anodic potentials (Table 2 with the Mo(II) and Mn(I) complexes) is less reflective of the precise electrochemical differences between these substances. Nevertheless, it can be confidently stated that for the Mo(II) and Fe(II) analogues, metal oxidation is significantly more difficult to affect if the Tp ligand includes a fluorinated phenyl substituent.

Table 2: Half-Cell and Peak Anodic Potentials (V)[a]

9	0.23[b,c]	this work
10	0.25[b,c]	this work
$(PhBpz_3)Mo(CO)_2$(2-methallyl)	0.16[d,e]	ref. 12
$(C_6F_5Bpz_3)Mo(CO)_2$(2-methallyl)	0.46[f,e]	ref. 12
11	0.75[b,e]	this work
12	0.77[b,e]	this work
$(PhBpz_3)Mn(CO)_3$	0.74[f,e]	ref. 12
$(C_6F_5Bpz_3)Mn(CO)_3$	0.84[f,e]	ref. 12
13	-0.21[b,g]	this work
14	-0.19[b,g]	this work
$(PhBpz_3)_2Fe$	-0.37[b,e]	ref. 12
$(C_6F_5Bpz_3)_2Fe$	-0.21[b,e]	ref. 12

[a](vs. $FeCp_2/[FeCp_2]^+$ in CH_2Cl_2), [b]Half-Cell Potential, [c](Scan rate = 0.1 V s^{-1}, $[NBu_4][B\{3,5\text{-}(CF_3)_2C_6H_3\}_4]$), [d]Quasireversible electron transition, [e](Scan rate = 0.1 V s^{-1}, $[NBu_4][B(C_6F_5)_4]$), [f]Irreversible electron transition (Peak Anodic E), [g](Scan rate = 0.1 V s^{-1}, $[NBu_4][BPh_4]$)

While the extents of the anodic shifts between the phenyltris(pyrazol-1-yl)borate complex and the most difficult fluorinated complex to oxidize within each analogous series are modest (Mo(II) allyl complexes: ~0.30 V; Mn; Fe(II) complexes: ~0.18 V), consideration of all redox tuning opportunities is important since small molecule activation supported by Tp ligands often involves oxidation-reduction steps. The Table 2 potentials for the Mn(I) complexes are most similar, spanning a range of only ~0.10 V. It is intriguing that the ranking of these voltages varies within each analogous set. For example, while $(C_6F_5Bpz_3)Mo(CO)_2$(2-methallyl) is ~0.30 V more difficult to oxidize than $(PhBpz_3)Mo(CO)_2$(2-methallyl), these differences for 3,5-

bis(trifluoromethyl)phenyl **10** (~0.09 V) the 3,4,5-trifluorophenyl **9** (~0.07 V) are similarly smaller; perfluorophenyltris(pyrazol-1-yl)borate is clearly the best ligand of this series to render its PhTpMo$(CO)_2$(2-methallyl) analogue easiest to reduce. In contrast, bis[3,5-bis(trifluoromethyl)phenyl] **14** is the most difficult to oxidize of the iron(II) analogues, with a half-cell potential ~0.18 V greater than that of $(PhBpz_3)_2Fe$. In this ferrous set, the perfluorophenyl and 3,4,5-trifluorophenyl borates are not distinguished, with half-cell potentials both ~0.16 V more positive than that of $(PhBpz_3)_2Fe$. The manganese data suggest that **11** is more difficult to oxidize than $(PhBpz_3)Mn(CO)_3$ but these data are difficult to directly compare since **11** exhibits reversibility ($E_{1/2}$ = 0.75 V) while $(PhBpz_3)Mn(CO)_3$ was reported to exhibit an irreversible wave (E_{pa} = 0.74 V), with the same experimental conditions and scan rate. These electrochemical data suggest that the extent of phenyl substituent fluorination necessary to minimize metal center electron-richness in phenyltris(pyrazol-1-yl)borate complexes cannot be confidently predicted in advance but that 3,4,5-trifluorophenyl-, 3,5-bis(trifluoromethyl)phenyl- and perfluorophenyltris(pyrazol-1-yl)borates affect metal center electronics similarly.

Closing Remarks

The importance of electron deficient Tp ligands for metal center tuning motivates the introduction of electron-withdrawing substituents into the scorpionate framework. While the implementation of fluorinated pyrazolyl groups offers the most direct approach, the possibility of modulating donation into κ^3-*N,N,N* bound metals via fluorination of the nondonor phenyl group of phenyltris(pyrazol-1-yl)borates has only recently been examined. Wagner has shown that perfluorophenyltris(pyrazol-1-yl)borates affect significant anodic shifts in half-cell potentials in their metal complexes relative those of phenyltris(pyrazol-1-yl)borate analogues. This study shows that 3,4,5-trifluorophenyl- and 3,5-bis(trifluoromethyl)phenyl(pyrazol-1-yl)borates affect similar anodic shifts within their metal complexes, with coordination of bis-CF_3

scorpionates consistently rendering metal centers slightly more difficult to oxidize. It is particularly interesting that the half-cell potential of $Fe(((3,5\text{-}CF_3)C_6H_3)Bpz_3)_2$ is more positive than that measured for $Fe(C_6F_5Bpz_3)_2$. Whether a similar electronic impact can be assessed in monoscorpionate iron(II) complexes that are candidates for small molecule activation studies is under investigation in this laboratory.

Experimental

Similar procedures were conducted to synthesize each analogous pair containing 3,4,5-trifluorophenyl and 3,5-bis(trifluoromethyl)phenyl substituents. Representative procedures for the 3,4,5-trifluorophenyl species are provided below. General procedures, experimental details, spectra (NMR, IR) and cyclic voltammograms are in the ESI.

$((3,4,5\text{-}F)C_6H_2)B(NMe_2)_2$ (1)

Neat $BrB(NMe_2)_2$ (9.758 g, 54.6 mmol) was added to a solution of $((3,4,5\text{-}F)C_6H_2)MgBr$ (freshly prepared from 5-bromo-1,2,3-trifluorobenzene (11.509 g, 54.6 mmol) and magnesium (1.352 g, 55.6 mmol)) in Et_2O (40 mL) at 0 °C. The brown mixture was stirred for 1 hr at 0 °C, and for another 14 hr at ambient temperature. The mixture separated into a two-phase system with a more dense brown layer and a pale yellow upper layer. The solvent was nearly completely removed *in vacuo* with the mixture maintained between 0 °C and -10 °C. Pentane (75 mL) was added to extract a pale yellow solution from a tan solid; the solid (containing $MgBr_2$) was separated by filtration. Roughly two-thirds of the filtrate volume was removed in vacuo with the solution maintained between 0°C and -10 °C. The concentrated filtrate was distilled (82-84 °C, 3 torr) to afford an air sensitive colorless liquid (9.148 g, 39.8 mmol, 73%). ^{11}B NMR (128 MHz, C_6D_6): δ 31.3 (s). $^{19}F\{^1H\}$ NMR (376 MHz, C_6D_6): δ -136.6 (d, $^3J_{FF}$ = 20.3 Hz, *m*-F), -162.6 (t, $^3J_{FF}$ = 20.3 Hz, *p*-F). ^1H NMR (400 MHz, C_6D_6): δ 6.71 (m, 2H, *o*-H), 2.37 (s, 12H, Me). $^{13}C\{^1H\}$ NMR (101 MHz, C_6D_6): δ 151.9 (dd, $^1J_{CF}$ = 250 Hz, $^2J_{CF}$ = 9.4 Hz, *m*-C), 140.1 (dt, $^1J_{CF}$ = 250

Hz, $^{2}J_{CF}$ = 15.4 Hz, *p*-F), 117.2 (dd, $^{2}J_{CF}$ = 13.3 Hz, $^{3}J_{CF}$ = 4.4 Hz, *o*-C), 50.0 (s, Me), *i*-C not observed.

((3,5-CF$_3$)C$_6$H$_3$)B(NMe$_2$)$_2$ (2)

Yield = 83% (air sensitive colorless liquid). Bp. 75-77 °C, 3 torr. ^{11}B NMR (128 MHz, C_6D_6): δ 31.3 (s). ^{19}F{^{1}H} NMR (376 MHz, C_6D_6): δ -62.6 (s, CF_3). ^{1}H NMR (400 MHz, C_6D_6): δ 7.82 (s, br, 1H, *p*-H), 7.73 (s, br, 2H, *o*-H), 2.31 (s, 12H, Me). ^{13}C{^{1}H} NMR (101 MHz, C_6D_6): δ 145.3 (s, br, *i*-C), 134.1 (m, *o*-C), 131.3 (q, $^{2}J_{CF}$ = 32.6 Hz, *m*-C), 124.9 (q, $^{1}J_{CF}$ = 270 Hz, CF_3), 122.0 (septet, $^{3}J_{CF}$ = 4.0 Hz, p-C), 40.9 (s, Me).

K[((3,4,5-F)C$_6$H$_2$)Bpz$_3$] (3)

Toluene (245 mL) and THF (95 mL) were added to **1** (6.93 g, 30.1 mmol) and pyrazole (4.142 g, 60.8 mmol); the resulting clear and colorless solution was stirred for 150 min. This solution was added to potassium pyrazolate (3.23 g, 30.4 mmol). The ambient temperature suspension was heated to reflux (8 hr) affording a clear and colorless solution. The solvent was removed *in vacuo*, while maintaining the temperature at 40 °C, revealing a white solid. After drying *in vacuo* at ambient temperature (1.5 hr), pentane (125 mL) was added and the white solid was separated from a colorless filtrate. The solid was washed with pentane (4 * 25 mL) and dried *in vacuo* (6 hr). The white solid (11.41 g) containing toluene was heated in a Schlenk tube *in vacuo* via an oil bath (120 °C, 24 hr) and massed as a nearly solvent-free white salt (10.47 g, 91%). Anal. Calcd for $C_{15}H_{11}BF_3KN_6$: C, 47.14; H, 2.90; N, 21.99. Found: C, 47.28; H, 2.59; N, 21.85. Mp: 210 - 212 °C (dec). ^{11}B NMR (128 MHz, DMSO-d^6): δ 0.71 (s). ^{19}F{^{1}H} NMR (376 MHz, DMSO-d^6): δ -140.4 (d, $^{3}J_{FF}$ = 21.3 Hz, *m*-F), -167.9 (t, $^{3}J_{FF}$ = 21.3 Hz, *p*-F). ^{1}H NMR (400 MHz, DMSO-d^6): δ 7.49 (m, 3H, pzH-3/-5), 7.23 (m, 2H, *o*-H), 6.75 (d, *J* = 2.0 Hz, 3H, pz-3/-5), 6.07 (app. t, *J* = 1.8 Hz, 3H, pzH-4). ^{13}C{^{1}H} NMR (101 MHz, DMSO-d^6): δ 148.7 (dd, $^{1}J_{CF}$ =

240 Hz, $^{2}J_{CF}$ = 9.0 Hz, m-C), 139.1 (s, pzC-3/-5), 136.6 (dt, $^{1}J_{CF}$ = 240 Hz, $^{2}J_{CF}$ = 16.0 Hz, *p*-F), 133.2 (s, pzC-3/-5), 117.2 (dd, $^{2}J_{CF}$ = 14.1 Hz, $^{3}J_{CF}$ = 2.7 Hz, *o*-C), 102.9 (s, pzC-4), *i*-C not observed.

K[((3,5-CF$_3$)C$_6$H$_3$)Bpz$_3$] (4)

Yield = 93% (white solid). Anal. Calcd for $C_{17}H_{12}BF_6KN_6$: C, 43.98; H, 2.61; N, 18.10. Found: C, 44.12; H, 2.50; N, 18.30. Mp: 177 - 178 °C (dec). ^{11}B NMR (128 MHz, DMSO-d^6): δ 0.95 (s). ^{19}F{^{1}H} NMR (376 MHz, DMSO-d^6): δ -60.9 (s, CF$_3$). ^{1}H NMR (400 MHz, DMSO-d^6): δ 8.19 (s, br, 2H, *o*-H), 7.72 (s, br, 1H, *p*-H), 7.52 (app. d, *J* = 0.89 Hz, 3H, pzH-3/-5), 6.73 (app. d, *J* = 1.8 Hz, 3H, pzH-3/-5), 6.10 (t, *J* = 2.0 Hz, 3H, pzH-4). ^{13}C{^{1}H} NMR (101 MHz, DMSO-d^6): δ 153.3 (s, br, *i*-C), 139.3 (s, pzC-3/-5), 134.5 (m, *o*-C), 133.2 (s, pzC-3/-5), 127.1 (q, $^{2}J_{CF}$ = 31.4 Hz, *m*-C), 124.9 (q, $^{1}J_{CF}$ = 273 Hz, CF$_3$), 118.4 (septet, $^{3}J_{CF}$ = 3.8 Hz, p-C), 103.1 (s, pzC-4).

Tl[((3,4,5-F)C$_6$H$_2$)Bpz$_3$] (5)

THF (30 mL) was added to **3** (0.463 g, 1.21 mmol) and thallium acetate (0.351 g, 1.33 mmol). The suspension was stirred at ambient temperature for 24 hr. The mixture was filtered through a plug of Celite separating a white solid from a colorless filtrate. Removal of the solvent *in vacuo* revealed a white solid that was dried in vacuo for 4 hr (0.496 g, 75%). Anal. Calcd for $C_{15}H_{11}BF_3N_6Tl$: C, 32.91; H, 2.03; N, 15.35. Found: C, 33.00; H, 2.01; N, 14.99. Mp: 230 - 231 °C (dec). ^{11}B NMR (128 MHz, C$_4$D$_8$O): δ 0.94 (s). ^{19}F{^{1}H} NMR (376 MHz, C$_4$D$_8$O): δ -138.0 (d, $^{3}J_{FF}$ = 19.8 Hz, *m*-F), -165.2 (t, $^{3}J_{FF}$ = 20.1 Hz, *p*-F). ^{1}H NMR (400 MHz, C$_4$D$_8$O): δ 7.59 (d, *J* = 1.5 Hz, 3H, pzH-3/-5), 7.35 (d, *J* = 2.2 Hz, 3H, pzH-3/-5), 6.47 (m, 2H, *o*-H), 6.20 (t, *J* = 2.0 Hz, 3H, pzH-4). ^{13}C{^{1}H} NMR (101 MHz, C$_4$D$_8$O): δ 151.8 (dd, $^{1}J_{CF}$ = 250 Hz, $^{2}J_{CF}$ = 9.0 Hz, *m*-C), 140.7 (s, pzC-3/-5), 139.8 (dt, $^{1}J_{CF}$ = 250 Hz, $^{2}J_{CF}$ = 15.7 Hz, *p*-F), 136.7 (s, pzC-3/-5), 117.8 (dd, $^{2}J_{CF}$ = 13.7 Hz, $^{3}J_{CF}$ = 4.2 Hz, *o*-C), 104.7 (s, pzC-4), *i*-C not observed.

Tl[((3,5-CF_3)C_6H_3)Bpz_3] (6)

Yield = 60% (white solid). Anal. Calcd for $C_{17}H_{12}BF_6N_6Tl$: C, 32.44; H, 1.92; N, 13.35. Found: C, 32.75; H, 1.80; N, 13.09. Mp: 177 - 178 °C (dec). ^{11}B NMR (128 MHz, C_4D_8O): δ 1.17 (s). $^{19}F\{^1H\}$ NMR (376 MHz, C_4D_8O): δ -63.2 (s, CF_3). ^1H NMR (400 MHz, C_4D_8O): δ 7.88 (s, br, 1H, *p*-H), 7.61 (m, 3H, pzH-3/-5), 7.37 (s, br, 2H, *o*-H), 7.32 (m, pzH-3/-5), 6.22 (m, 3H, pzH-4). $^{13}C\{^1H\}$ NMR (101 MHz, C_4D_8O): δ 141.0 (s, pzC-3/-5), 134.6 (m, *o*-C), 136.7 (s, pzC-3/-5), 131.0 (q, $^2J_{CF}$ = 32.4 Hz, *m*-C), 125.1 (q, $^1J_{CF}$ = 273 Hz, CF_3), 121.8 (septet, $^3J_{CF}$ = 3.8 Hz, *p*-C), 105.0 (s, pzC-4), *i*-C not observed.

[Et_4N][$Mo(CO)_3$(((3,4,5-F)C_6H_2)Bpz_3)] (7)

THF (50 mL) was added to **3** (0.465 g, 1.22 mmol) and $Mo(CO)_3(CH_3CH_2CN)_3$ (0.400 g, 1.16 mmol). The yellow solution was refluxed (1.5 hr), transferred to Et_4NBr (0.268 g, 1.27 mmol) and stirred at ambient temperature (2 hr) before the solvent was removed in vacuo. The residue was dissolved in CH_3CN (40 mL) and the solution was filtered through alumina. Most of the solvent from the pale yellow filtrate was removed in vacuo revealing a yellow solid. Addition of Et_2O (30 mL) resulted in a suspended pale yellow solid that was isolated by filtration, washed with Et_2O (3 * 10 mL) and dried in vacuo for 2 hr. Et_2O diffusion into a CH_3CN solution provided yellow microcrystals (0.501 g, 66%). Anal. Calcd for $C_{26}H_{31}BF_3MoN_7O_3$: C, 47.80; H, 4.78; N, 15.01. Found: C, 47.71; H, 4.53; N, 14.85. Mp: 303 - 305 °C (dec). IR (CH_3CN) ν_{max}(CO)/cm^{-1} 1894 (s), 1760 (s) cm^{-1}; (Nujol) ν_{max}(CO)/cm^{-1} 1892 (s), 1760 (s, sh), 1743 (s) cm^{-1}. ^{11}B NMR (128 MHz, CD_3CN): δ -0.77 (s). $^{19}F\{^1H\}$ NMR (376 MHz, CD_3CN): δ -137.3 (d, $^3J_{FF}$ = 19.7 Hz, *m*-F), -164.1 (t, $^3J_{FF}$ = 19.7 Hz, *p*-F). ^1H NMR (400 MHz, CD_3CN): δ 7.82 (m, 3H, pzH-3/-5), 7.62 (m, 2H, *o*-H), 7.47 (d, *J* = 2.4 Hz, 3H, pz-3/-5), 6.12 (app. t, *J* = 2.2 Hz, 3H, pzH-4), 3.11 (m, 8H, Et_4N), 1.17 (m, 12H, Et_4N). $^{13}C\{^1H\}$ NMR (101 MHz, CD_3CN): δ 231.8 (s, CO), 151.9

(dd, $^{1}J_{CF}$ = 251 Hz, $^{2}J_{CF}$ = 6.1 Hz, *m*-C), 145.1 (s, pzC-3/-5), 140.4 (dt, $^{1}J_{CF}$ = 251 Hz, $^{2}J_{CF}$ = 15.4 Hz, *p*-F), 135.9 (s, pzC-3/-5), 120.0 (dd, $^{2}J_{CF}$ = 14.6 Hz, $^{3}J_{CF}$ = 5.1 Hz, *o*-C), 105.6 (s, pzC-4), 53.2 (m, Et_4N), 7.7 (s, Et_4N), *i*-C not observed.

[Et_4N][$Mo(CO)_3$(((3,5-CF_3)C_6H_3)Bpz_3)] (8)

Yield = 51% (off-white solid). Anal. Calcd for $C_{28}H_{32}BF_6MoN_7O_3$: C, 45.73; H, 4.39; N, 13.33. Found: C, 45.79; H, 4.05; N, 13.14. Mp: 260 - 261 °C (dec). IR (CH_3CN) ν_{max}(CO)/cm^{-1} 1895 (s), 1761 (s) cm^{-1}; (THF) ν_{max}(CO)/cm^{-1} 1892 (s), 1762 (s), 1750 cm^{-1} (s, sh); (Nujol): ν_{max}(CO)/cm^{-1} 1894 (s), 1769 (s), 1749 (s), 1745 (s, sh) cm^{-1}. ^{11}B NMR (128 MHz, CD_3CN): δ -0.52 (s). ^{19}F{^{1}H} NMR (376 MHz, CD_3CN): δ -63.1 (s, CF_3). ^{1}H NMR (400 MHz, CD_3CN): δ 8.46 (s, br, 2H, *o*-H), 8.16 (s, br, 1H, *p*-H), 7.85 (app. d, *J* = 1.8 Hz, 3H, pzH-3/-5), 7.38 (app. d, *J* = 2.4 Hz, pzH-3/-5), 6.14 (t, *J* = 2.2 Hz, 3H, pzH-4), 3.10 (m, 8H, Et_4N), 1.16 (m, 12H, Et_4N). ^{13}C{^{1}H} NMR (101 MHz, CD_3CN): δ 231.8 (s, CO), 153.3 (s, br, *i*-C), 145.3 (s, pzC-3/-5), 136.0 (s, br, *o*-C), 135.9 (s, pzC-3/-5), 131.5 (q, $^{2}J_{CF}$ = 32.8 Hz, m-C), 125.1 (q, $^{1}J_{CF}$ = 273 Hz, CF_3), 123.2 (septet, $^{3}J_{CF}$ = 3.7 Hz, p-C), 105.8 (s, pzC-4), 53.1 (m, Et_4N), 7.7 (s, Et_4N), *i*-C not observed.

(((3,4,5-F)C_6H_2)Bpz_3)$Mo(CO)_2$(2-methallyl) (9)

A 1.00 mL stock solution of 2-methylallyl bromide (0.230 g, 1.70 mmol) in CH_2Cl_2 was added to $Mo(CO)_3(C_5H_5N)_3$ (0.645 g, 1.55 mmol) in CH_2Cl_2 (20 mL). The reaction mixture was stirred (3 hr) while its color changed from yellow to pale orange; an IR spectrum ((CH_2Cl_2) ν_{max}(CO)/cm^{-1} 1938 (s), 1835 (m) cm^{-1}) indicated complete consumption of $Mo(CO)_3(C_5H_5N)_3$ and $Mo(CO)_2(C_5H_5N)_2$(2-methallyl)Br formation. This orange solution was added (along with a 10 mL CH_2Cl_2 rinse of the $Mo(CO)_2(C_5H_5N)_2$(2-methallyl)Br flask) to **3** (0.644 g, 1.70 mmol). The yellow suspension was stirred (16 hr) and then filtered through alumina. The CH_2Cl_2 was

removed *in vacuo*, and the yellow solid was suspended in pentane (50 mL). This solid was collected by filtration, washed with pentane (3 * 10 mL) and dried *in vacuo* (6 hr). The solid was dissolved in THF (20 mL) and the yellow solution was filtered through alumina. The filtrate solvent was removed in vacuo revealing a yellow solid (0.498 g, 59%) that was suspended in pentane (30 mL), isolated by filtration, washed with pentane (3 * 10 mL) and dried *in vacuo* (5 hr). Anal. Calcd for $C_{21}H_{18}BF_3MoN_6O_2$: C, 45.85; H, 3.30; N, 15.28. Found: C, 45.85; H, 3.24; N, 15.20. Mp: 229 - 231 °C (dec). IR (CH_2Cl_2) ν_{max}(CO)/cm^{-1} 1943 (s), 1851 (s) cm^{-1}; (THF) ν_{max}(CO)/cm^{-1} 1944 (s), 1857 (s); (Nujol) ν_{max}(CO)/cm^{-1} 1941 (s), 1851 (s). ^{11}B NMR (128 MHz, C_4D_8O): δ -1.20 (s). ^{19}F{^{1}H} NMR (376 MHz, C_4D_8O): δ -136.3 (d, $^3J_{FF}$ = 20.4 Hz, *m*-F), -163.4 (t, $^3J_{FF}$ = 20.3 Hz, *p*-F). ^{1}H NMR (400 MHz, C_4D_8O): δ 8.24 (s, br, 3H, pzH-3/-5), 7.61 (m, 2H, *o*-H), 7.35 (s, br, 3H, pz-3/-5), 6.24 (s, 3H, pzH-4), 3.60 (s, 2H, allyl-CHH), 1.64 (s, 3H, allyl-CH_3), 1.34 (s, 2H, allyl-CHH). ^{13}C{^{1}H} NMR (101 MHz, C_4D_8O): δ 228.2 (s, CO), 152.1 (dd, $^1J_{CF}$ = 251 Hz, $^2J_{CF}$ = 6.4 Hz, *m*-C), 145.2 (s, br, pzC-3/-5), 140.5 (dt, $^1J_{CF}$ = 253 Hz, $^2J_{CF}$ = 15.4 Hz, *p*-F), 137.8 (s, br, pzC-3/-5), 119.8 (dd, $^2J_{CF}$ = 14.6 Hz, $^3J_{CF}$ = 5.2 Hz, *o*-C), 106.3 (s, pzC-4), 84.1 (s, CCH_3), 59.8 (s, allyl-CH_2), 18.9 (s, allyl-CH_3), *i*-C not observed.

(((3,5-CF_3)C_6H_3)Bpz_3)Mo(CO)$_2$(2-methallyl) (10)

Yield = 51% (bright yellow solid). Anal. Calcd for $C_{23}H_{19}BF_6MoN_6O_2$: C, 43.70; H, 3.03; N, 13.29. Found: C, 43.30; H, 2.66; N, 12.91. Mp: 232 - 234 °C (dec). IR (CH_2Cl_2) ν_{max}(CO)/cm^{-1} 1943 (s), 1851 (m) cm^{-1}; (THF) ν_{max}(CO)/cm^{-1} 1945 (s), 1857 (s); (Nujol) ν_{max}(CO)/cm^{-1} 1935 (s), 1842 (s). ^{11}B NMR (128 MHz, C_4D_8O): δ -0.97 (s). ^{19}F{^{1}H} NMR (376 MHz, C_4D_8O): δ -63.5 (s, CF_3). ^{1}H NMR (400 MHz, C_4D_8O): δ 8.45 (s, br, 2H, *o*-H), 8.29 (s, br, 3H, pzH-3/-5), 8.19 (s, br, 2H, *p*-H), 7.27 (s, br, 3H, pz-3/-5), 6.27 (s, 3H, pzH-4), 3.62 (s, 2H, allyl-CHH), 1.66 (s, 3H, allyl-CH_3), 1.36 (s, 2H, allyl-CHH). ^{13}C{^{1}H} NMR (101 MHz, C_4D_8O): δ 228.2 (s, CO), 145.2 (s,

br, pzC-3/-5), 137.7 (s, br, pzC-3/-5), 135.7 (m, *o*-C), 132.0 (q, $^2J_{CF}$ = 32.8 Hz, *m*-C), 124.9 (q, $^1J_{CF}$ = 274 Hz, CF_3), 123.2 (septet, $^3J_{CF}$ = 3.8 Hz, *p*-C), 106.6 (s, pzC-4), 84.2 (s, CCH_3), 59.9 (s, allyl-CH_2), 19.0 (s, allyl-CH_3), *i*-C not observed.

(((3,4,5-F)C_6H_2)Bpz$_3$)Mn(CO)$_3$ (11)

THF (50 mL) was added to solid [Mn($C_{10}H_8$)(CO)$_3$][BF_4] (0.441 g, 1.25 mmol) and **3** (0.500 g, 1.31 mmol); the colorless solution was stirred (16 hr) and then filtered through alumina. The solvent of the filtrate was removed in vacuo. Pentane (30 mL) was added and the colorless solution was cooled to -25 °C. The resulting suspension was filtered while maintaining the temperature between -30 °C and -25 °C to separate an ivory solid from a colorless filtrate. This solid (0.405 g, 67%) was washed with cold (-25 °C) pentane (4 * 10 mL) and dried *in vacuo* for 8.5 hr. Anal. Calcd for $C_{18}H_{11}BF_3MnN_6O_3$: C, 44.85; H, 2.30; N, 17.43. Found: C, 43.99; H, 0.64; N, 16.66. Mp: 223 - 225 °C (dec). IR (CH_2Cl_2) ν_{max}(CO)/cm^{-1} 2036 (s), 1933 (s); (THF) ν_{max}(CO)/cm^{-1} 2036 (s), 1933 (s); (Nujol) ν_{max}(CO)/cm^{-1} 2032 (s), 1936 (s), 1923 (s, sh). ^{11}B NMR (128 MHz, C_4D_8O): δ -1.5 (s). ^{19}F{^{1}H} NMR (376 MHz, C_4D_8O): δ -136.2 (d, $^3J_{FF}$ = 20.4 Hz, *m*-F), -163.1 (t, $^3J_{FF}$ = 20.1 Hz, *p*-F). ^{1}H NMR (400 MHz, C_4D_8O): 8.07 (m, 3H, pzH-3/-5), 7.68 (m, 5H, *o*-H, pz-3/-5), 6.30 (app. t, *J* = 2.2 Hz, 3H, pzH-4). ^{13}C{^{1}H} NMR (101 MHz, C_4D_8O): δ 222.3 (s, CO), 152.1 (dd, $^1J_{CF}$ = 249 Hz, $^2J_{CF}$ = 7.4 Hz, *m*-C), 146.2 (s, pzC-3/-5), 140.7 (dt, $^1J_{CF}$ = 253 Hz, $^2J_{CF}$ = 15.4 Hz, *p*-F), 136.9 (s, pzC-3/-5), 119.6 (dd, $^2J_{CF}$ = 14.7 Hz, $^3J_{CF}$ = 5.2 Hz, *o*-C), 106.9 (s, pzC-4), *i*-C not observed.

(((3,5-CF_3)C_6H_3)Bpz$_3$)Mn(CO)$_3$ (12)

Yield = 69% (ivory solid). Anal. Calcd for $C_{20}H_{12}BF_6MnN_6O_3$: C, 42.59; H, 2.14; N, 14.90. Found: C, 42.54; H, 0.24; N, 14.49. Mp: 221 - 223 °C (dec). IR (CH_2Cl_2) ν_{max}(CO)/cm^{-1} 2035 (s), 1932 (s); (THF) ν_{max}(CO)/cm^{-1} 2035 (s), 1932 (s); (Nujol) ν_{max}(CO)/cm^{-1} 2032 (s), 1934 (s),

1917 (s). ^{11}B NMR (128 MHz, C_4D_8O): δ -1.2 (s). ^{19}F{^{1}H} NMR (376 MHz, C_4D_8O): δ -63.5 (s, CF_3). ^{1}H NMR (400 MHz, C_4D_8O): δ 8.53 (s, br, 2H, *o*-H), 8.23 (s, br, 2H, *p*-H), 8.11 (m, 3H, pzH-3/-5), 7.59 (m, 3H, pz-3/-5), 6.32 (app. t, *J* = 2.3 Hz, 3H, pzH-4). ^{13}C{^{1}H} NMR (101 MHz, C_4D_8O): δ 222.3 (s, CO), 146.4 (s, pzC-3/-5), 136.7 (s, pzC-3/-5), 135.7 (m, *o*-C), 132.1 (q, $^2J_{CF}$ = 32.8 Hz, *m*-C), 124.9 (q, $^1J_{CF}$ = 274 Hz, CF_3), 123.5 (septet, $^3J_{CF}$ = 3.8 Hz, *p*-C), 107.2 (s, pzC-4), *i*-C not observed.

Fe(((3,4,5-F)C_6H_2)Bpz_3)$_2$ (13)

THF (15 mL) was added to anhydrous $FeCl_2$ (0.075 g, 0.592 mmol) and **3** (0.452 g, 1.18 mmol). The mixture was stirred 18 hr and became red-violet. More THF was added (10 mL), and the suspension was filtered through alumina. The solvent from the red-violet filtrate was removed *in vacuo* revealing a pale red solid. Pentane (30 mL) was added and the solid (0.258 g, 59%) was isolated by filtration, washed with pentane (3 * 5 mL) and dried in vacuo (6 hr). Anal. Calcd for $C_{30}H_{22}B_2F_6FeN_{12}$: C, 48.56; H, 2.99; N, 22.65. Found: C, 47.69; H, 2.42; N, 22.19. Mp: 300 - 301 °C (dec). ^{11}B NMR (128 MHz, C_4D_8O): δ -1.4 (s). ^{19}F{^{1}H} NMR (376 MHz, C_4D_8O): δ -136.8 (d, $^3J_{FF}$ = 20.3 Hz, *m*-F), -163.7 (t, $^3J_{FF}$ = 20.3 Hz, *p*-F). ^{1}H NMR (400 MHz, C_4D_8O) δ 7.93 (m, 6H, pzH-3/-5), 7.88 (app. t, *J* = 8.1 Hz, 4H, *o*-H), 6.99 (s, br, 6H, pz-3/-5), 6.35 (s, br, 6H, pzH-4). ^{13}C{^{1}H} NMR (101 MHz, C_4D_8O): δ 152.3 (dd, $^1J_{CF}$ = 250 Hz, $^2J_{CF}$ = 7.5 Hz, *m*-C), 151.7 (s, pzC-3/-5), 140.7 (dt, $^1J_{CF}$ = 252 Hz, $^2J_{CF}$ = 15.3 Hz, *p*-F), 140.4 (s, pzC-3/-5), 119.9 (dd, $^2J_{CF}$ = 14.6 Hz, $^3J_{CF}$ = 4.8 Hz, *o*-C), 108.5 (s, pzC-4), *i*-C not observed.

Fe(((3,5-CF_3)C_6H_3)Bpz_3)$_2$ (14)

Yield = 53% (pale red solid). Anal. Calcd for $C_{34}H_{24}B_2F_{12}FeN_{12}$: C, 45.07; H, 2.67; N, 18.55. Found: C, 44.78; H, 2.73; N, 17.97. Mp: 307 - 308 °C (dec). ^{11}B NMR (128 MHz, C_4D_8O): δ -1.3 (s). ^{19}F{^{1}H} NMR (376 MHz, C_4D_8O): δ -63.3 (s, CF_3). ^{1}H NMR (400 MHz, C_4D_8O): δ 8.73

(s, 4H, *o*-H), 8.27 (s, 2H, *p*-H), 7.87 (s, 6H, pzH-3/-5), 7.11 (s, 6H, br, pz-3/-5), 6.44 (s, 6H, pzH-4). $^{13}C\{^1H\}$ NMR (101 MHz, C_4D_8O): δ 152.6 (s, pzC-3/-5), 140.8 (s, pzC-3/-5), 135.8 (m, *o*-C), 131.9 (q, $^2J_{CF}$ = 32.7 Hz, *m*-C), 125.1 (q, $^1J_{CF}$ = 274 Hz, CF_3), 123.2 (m, *p*-C), 109.1 (s, pzC-4), *i*-C not observed.

$Cu(((3,4,5\text{-}F)C_6H_2)Bpz_3)_2$ (15)

THF (25 mL) was added to anhydrous $CuBr_2$ (0.175 g, 0.785 mmol) and **3** (0.600 g, 1.57 mmol); the dark blue mixture was stirred for 16 hr. The THF was removed in vacuo, and the blue residue was dissolved in CH_2Cl_2 (25 mL). The solution was filtered through alumina, and the solvent was removed *in vacuo*. Pentane (30 mL) was added to the pale blue solid that was isolated by filtration, washed with pentane (4 * 15 mL) and dried *in vacuo* (6 hr) (0.237 g, 40%). Anal. Calcd for $C_{30}H_{22}B_2CuF_6N_{12}$: C, 48.06; H, 2.96; N, 22.42. Found: C, 48.14; H, 1.13; N, 22.07. Mp: 251 - 253 °C (dec). No ^{11}B NMR resonance was observed (C_4D_8O). $^{19}F\{^1H\}$ NMR (376 MHz, C_4D_8O): δ -136.6 (s, *m*-F), -163.8 (s, *p*-F). μ_{eff} (C_4D_8O, method of Evans, 20 °C): 1.7 μ_B (S = ½).

$Cu(((3,5\text{-}CF_3)C_6H_3)Bpz_3)_2$ (16)

Yield = 43% (pale blue solid). Anal. Calcd for $C_{34}H_{24}B_2CuF_{12}N_{12}$: C, 44.69; H, 2.65; N, 18.39. Found: C, 44.54; H, 1.07; N, 18.07. Mp: 221 - 222 °C (dec). No ^{11}B NMR resonance was observed (C_4D_8O). $^{19}F\{^1H\}$ NMR (376 MHz, C_4D_8O): δ -63.2 (s, CF_3). μ_{eff} (C_4D_8O, method of Evans, 20 °C): 2.0 μ_B (S = ½).

X-ray Crystallography

X-ray quality crystals were obtained by diffusion of liquid heptane in CH_2Cl_2 solutions at -15 °C (**5**, **6**), diffusion of liquid Et_2O into CH_3CN solutions at 10 °C (**7**, **8**), evaporation of saturated pentane/CH_2Cl_2 solutions at ambient temperature (**9**, **10**) and evaporation of saturated

pentane/THF solutions at ambient temperature (**11**-**16**). These crystals were selected from the mother liquor in a N_2-filled glove bag and placed onto 0.15 mm diameter MiTeGen Dual-Thickness micro-loops. These crystals were mounted on a Bruker-AXS VENTURE diffractometer with a PHOTON-III CPAD detector (0.71073 Å Mo-Kα radiation) for data collection at 150(2) K. All structures were solved by direct methods using SHELXT-2018/2 and refined using SHELXT-2018/3.[20,21] All non-hydrogen atoms were placed in ideal positions and refined as riding atoms with relative isotropic displacement parameters. Further details of crystallographic data collection, solution, and refinement can be found in the ESI. Crystallographic CIF files for these structures: CCDC 2244249-2244260.

Cyclic Voltammetry

Cyclic voltammetry experiments of **9**, **10**, **13** and **14** were performed using a Pine Research Instrument WaveNow potentiostat with platinum screen-printed working and auxiliary electrodes and a Ag pseudo-reference on a ceramic substrate in CH_2Cl_2. Analyte solutions were prepared in 0.1 M solutions of tetrabutylammonium tetraphenylborate (**13**, **14**) and tetrabutylammonium tetrakis[3,5-bis(trifluoromethyl)phenyl]borate (**9**, **10**) and referenced internally to the $FeCp^*_2/[FeCp^*_2]^+$ redox couple at the end of each experiment. Cyclic voltammetry experiments of **11** and **12** were conducted using a CH Instruments Model CHI620D potentiostat using 0.05 M solutions of tetrabutylammonium tetrakis(perfluorophenyl)borate in CH_2Cl_2. The glassy carbon working electrode was polished with 1.0 mm and 0.25 mm diamond paste and rinsed with CH_2Cl_2 prior to use. A platinum wire was used as the counter electrode. The reference electrode was non-aqueous Ag/AgCl, that was separated from the solution by a porous frit. At the end of the experiments with **11** and **12**, 0.0019 g (0.010 mmol) of the ferrocene internal reference was added to the solutions.

Author Contributions

Conceptualization: P.J. Fischer; investigation: P.J. Fischer, C.B. Roe, J.N. Stephenson, R.J. Dunscomb, C.L. Carthy, C. Nataro, V.G. Young, Jr.; supervision: P.J. Fischer, C. Nataro; writing-original draft: P.J. Fischer.

Conflicts of interest

There are no conflicts of interest to declare.

Acknowledgments

The National Science Foundation (CHE-1954883) supported this research. The Bruker-AXS D8 Venture Photon-II diffractometer was purchased from an NSF-MRI grant (#1229400) and the University of Minnesota. P.J.F.is grateful to Prof. Ian A. Tonks (U of MN) for authorizing cyclic voltammetry work reported herein to be carried out in his laboratories and Alex Lovstedt (U of MN) for his X-ray crystallographic expertise.

References

1. P. J. Fischer, Polypyrazolylborates and Scorpionates (1.14). In *Compr. Coord. Chem. III*; E. C. Constable, G. Parkin, L. Que, Jr., Eds., Vol. 1, Elsevier, 2021; pp 428-504.

2. A. Noonikara-Poyil, S. G. Ridlen, I. Fernández, I.; H. V. R. Dias, *Chem. Sci.*, 2022, **13**, 7190.

3. G. Wang, A. Noonikara-Poyil, I. Fernández, H. V. R. Dias, *Chem. Commun.*, 2022, **58**, 3222.

4. S. G. Ridlen, J. Wu, N. V. Kulkarni, H. V. R. Dias, *Eur. J. Inorg. Chem.,* 2016, 2573.

5. N. B. Jayaratna, I. I. Gerus, R. V. Mironets, P. K. Mykhailiuk, M. Yousufuddin, H. V. R. Dias, *Inorg. Chem*., 2013, **52**, 1691.

6. H. V. R. Dias, S. A. Polach, S.-K. Goh, E. F. Archibong, D. S. Marynick, *Inorg. Chem*., 2000, **39**, 3894.

7. H. V. R. Dias, S. A. Polach, *Inorg. Chem*., 2000, **39**, 4676.

8. R. Gava, A. Olmos, B. Noverges, T. Varea, E. Álvarez, T. R. Belderrain, A. Caballero, G. Asensio, P. J. Pérez, *ACS Catal*., 2015, **5**, 3726.

9. N. V. Kulkarni, C. Dash, N. B. Jayaratna, S. G. Ridlen, S. K. Khani, A. Das, X. Kou, M. Yousufuddin, T. R. Cundari, H. V. R. Dias, *Inorg. Chem.,* 2015, **54**, 11043.

10. A. Loas, S. M. Gorun, *Eur. J. Inorg. Chem*., **2016**, 2648.

11. B. K. Muñoz, W.-S. Ojo, K. Jacob, N. Romero, L. Vendier, E. Despagnet-Ayoub, M. Etienne, *New J. Chem.*, 2014, **38**, 2451.

12. H. Vitze, M. Bolte, H.-W. Lerner, M. Wagner, *Eur. J. Inorg. Chem.,* 2016, 2443.

13. J. N. Bentley, S. A. Elgadi, J. R. Gaffen, P. Demay-Drouhard, T. Baumgartner, C. B. Caputo, *Organometallics,* 2020, **39**, 3645.

14. R. J. Blagg, T. R. Simmons, G. R. Hatton, J. M. Courtney, E. L. Bennett, E. J. Lawrence, G. G. Wildgoose, *Dalton Trans.*, 2016, **45**, 6032.

15. J. L. Kisko, T. Hascall, C. Kimblin, G. Parkin, *J. Chem. Soc., Dalton Trans.,* 1999, 1929.

16. E. R. Sirianni, G. P. A. Yap, K. H. Theopold, *Inorg. Chem.,* 2014, **53**, 9424.

17. A. J. Pearson, E. Schoffers, *Organometallics*, 1997, **16**, 5365.

18. H. V. R. Dias, H.-J. Kim, H.-L. Lu, K. Rajeshwar, N. R. de Tacconi, A. Derecskei-Kovacs, D. S. Marynick, *Organometallics*, 1996, **15**, 13, 2994.

19. A. Benchohra, Y. Li, L.-M. Chamoreau, B. Baptiste, E. Elkaïm, N. Guillou, D. Kreher, R. Lescouëzec, *Angew. Chem. Int. Ed.* 2021, **60**, 8803.

20. SHELXTL 2018, Bruker Analytical X-Ray Systems, Madison, WI (2018).

21. G. M. Sheldrick, *Acta Crystallogr., Sect. A: Fundam. Crystallogr.*, 2008, **64**, 112.